AR(1) time series with autoregressive gamma variance for road topography modeling

Johannesson, Pär; Podgorski, Krzysztof; Rychlik, Igor; Shariati Fokalaei, Nima

2015

Working Papers in Statistics
No 2015:5
Department of Statistics
School of Economics and Management
Lund University

AR(1) time series with autoregressive gamma variance for road topography modeling

PÄR JOHANNESSON, SP TECHNICAL RESEARCH INSTITUTE OF SWEDEN
KRZYSZTOF PODGÓRSKI, LUND UNIVERSITY
IGOR RYCHLIK, CHALMERS UNIVERSITY OF TECHNOLOGY
NIMA SHARIATI, LUND UNIVERSITY

AR(1) time series with autoregressive gamma variance for road topography modeling

PÄR JOHANNESSON*, KRZYSZTOF PODGÓRSKI**, IGOR RYCHLIK***, AND NIMA SHARIATI**@

* SP Technical Research Institute of Sweden, P.O. Box 24036, SE-400 22 Göteborg, Sweden
Par.Johannesson@sp.se

** Department of Statistics, Lund University, P.O. Box 743, SE-220 07 Lund, Sweden
krzysztof.podgorski@stat.lu.se
nima.shariati_fokalaei@stat.lu.se

*** Department of Mathematical Sciences, Chalmers University of Technology, SE-412 96 Göteborg, Sweden
rychlik@chalmers.se

@ Corresponding author

Abstract: A non-Gaussian time series with a generalized Laplace marginal distribution is used to model road topography. The model encompasses variability exhibited by a Gaussian AR(1) process with randomly varying variance that follows a particular autoregressive model that features the gamma distribution as its marginal. A simple estimation method to fit the correlation coefficient of each of two autoregressive components is proposed. The one for the Gaussian AR(1) component is obtained by fitting the frequency of zero crossing, while the autocorrelation coefficient for the gamma autoregressive process is fitted from the autocorrelation of the squared values of the model. The shape parameter of the gamma distribution is fitted using the explicitly given moments of a generalized Laplace distribution. Another general method of model fitting based on the correlation function of the signal is also presented and compared with the zero-crossing method. It is demonstrated that the model has the ability to accurately represent hilliness features of road topography providing a significant improvement over a purely Gaussian model.

Keywords: Non-Gaussian time series, gamma distributed variances, generalized Laplace distribution, road surface profile, road roughness, road hilliness.

1 Introduction

Modeling of road profiles is an active area of transportation engineering research. The road elevation consists of topography, roughness and texture. Texture is the high frequency components of a road profile responsible for noise, skid-resistance and tyre wear. Roughness is the road unevenness, containing wavelengths from about 0.1 m to 50 m, and cause vibration responses in the vehicle structure and components which may lead to fatigue problems. Variability of the roughness is often described by means of continuous random processes. This is then used to estimate risks of fatigue failures. Topography is the low frequency part of the elevation, corresponding to landscape variability, and is one of the most important factors in fuel consumption of utility vehicles. The topography can be described using slopes which are conveniently modeled by means of time series. The models are then used in dedicated programs to simulate fuel consumption of vehicles. The presented study was initiated by investigations of efficiency of different technical solutions to harvest energy from breaking and driving downhills of utility vehicles in mines. The empirical example that is used in this paper to illustrate the proposed model is based on topography records from a road surface segment in a mine. These data are presented in Figure 1.

Homogeneous Gaussian loads have been extensively studied in the literature and applied in models for road elevations. Early applications of Gaussian processes to model road surface roughness can be found in [7]. Direct Gaussian models are convenient since linear filter responses to them are Gaussian processes as well. However, the authors of that pioneering paper were aware that Gaussian processes cannot "exactly reproduce the profile of a real road". Although models based on Gaussian distributions are standard in the field (see, e.g., [17] and also [14] for some recent studies), most experts of vehicle engineering agree that road surfaces are not, in fact, accurately represented by a Gaussian distribution.

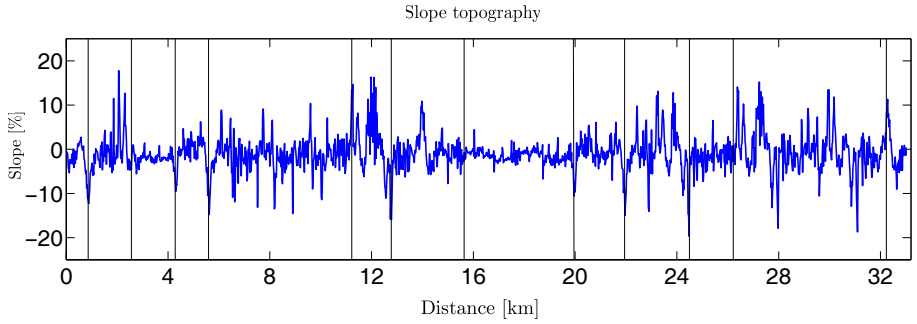

Figure 1: Empirically measured slopes expressed in percentage collected over a 33 km long segment of rough road surface. Vertical lines divide the records into apparently homogeneous variance sections.

One reason for this is that the actual roads contain short sections with above-average irregularity. As shown in [3], such irregularities cause most of the vehicle fatigue damage.

In [6], a non-homogeneous model is constructed as a sequence of independent Gaussian processes of varying variances but with the same standardized spectrum. This approach was further developed in [5, 15]. The variability of variances was modeled by a discrete distribution taking a few values. Another approach has been proposed in [2] where a bivariate road model was constructed based on a Gaussian process with added random irregularities. These types of models were further developed in [4], [13], [9] and [8] resulting in the so-called generalized Laplace models which, roughly, means that the variable variances are assumed to follow a gamma distribution.

This work focuses on autoregressive gamma variance AR(1) models which are classical Gaussian AR(1) processes modulated by autoregressive gamma distributed variances. Those are defined by only five parameters: mean, variance, kurtosis and two parameters defining autoregressive recursions. As an illustration, we use the model to describe variability of slopes encountered by a heavy duty vehicle transporting ore in a mine. Let us note here that our model easily generalizes by taking autoregressive gamma variances together with an arbitrary Gaussian time series. Hence it can be an alternative to Gaussian modes with a more complex correlation structure.

This paper is organized as follows. Firstly, the Laplace distribution is reviewed in Section 2. Then, the fundamentals of the proposed models are presented in Section 3. The dependence structure of the models through autocorrelation functions is presented in Section 4, while descriptions of model fitting procedures are given in Section 5. In Section 6, analysis of the road slopes is performed based on the model. An algorithm for simulation of autoregressive gamma variance AR(1) time series is finally described in Section 7.

2 Random variance model and generalized Laplace distribution

Frequently, in the distribution of real data, one observes heavier than normal tails. One way of accounting for this effect is by introducing a random variance varying over segments of the records. For example, for more heavily tailed data presented in Figure 1, we observe different variability over different sections of the record marked by vertical lines in this graph. This 'varying variability' can be observed on different horizontal scales and it was well documented in the road roughness data, see [13] and [4]. This variable local variance can be assumed to follow a certain distribution and, for example, the gamma distribution appeared to fit road elevation data quite well. In the simplest case, these gamma variables on disjoint segments of the roads could be viewed as independent variables. Since the sampling step is shorter than the length of a section with almost constant variance, each section can be modeled by stationary Gaussian autoregressive model. By combining a Gaussian model with a gamma distributed variance, we can account for the observed non-Gaussianity of the data. In fact, the resulting distribution will follow the generalized (symmetric) Laplace distribution. It follows from the following

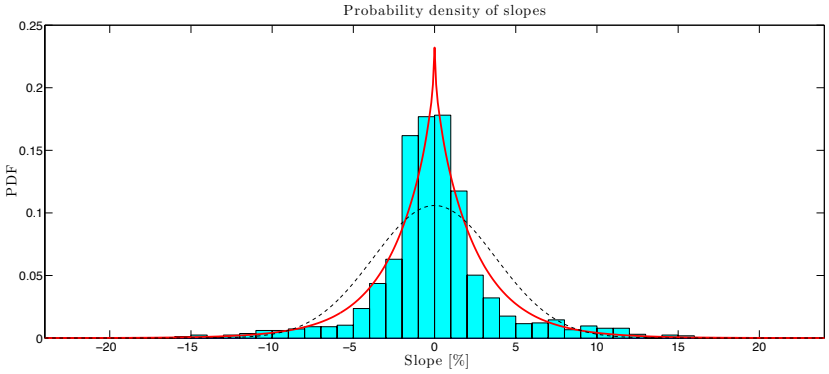

Figure 2: Models of slopes pdf; the Gaussian pdf $N(0, 14.18)$ (dashed line), the generalized Laplace pdf defined in (1) with parameters $m = 0$, $\nu = 1.108$, $\sigma^2 = 14.18$ (solid line) and the normalized histogram.

representation of a generalized Laplace variable

$$Y = \sigma\sqrt{R}X + m, \tag{1}$$

where X the standard normal (Gaussian) distribution and is independent of gamma distributed factor R that has mean one and variance ν defined by the density function

$$f(r) = \frac{1}{\Gamma\left(1/\nu\right)\nu^{1/\nu}}\, r^{\frac{1}{\nu}-1}e^{-r/\nu}, \tag{2}$$

where $\Gamma(\cdot)$ is the gamma function. The non-Gaussianity (shape) parameter ν can be estimated using

$$\nu = \frac{\kappa - 3}{3}, \tag{3}$$

where κ is the kurtosis, which for the Gaussian case is $\kappa = 3$. This parameter has a simple interpretation as the excess of kurtosis ($\kappa - 3$) measured in terms of the Gaussian kurtosis. Note also that if the non-Gaussianity parameter ν tends to zero, the random variance R converges (in distribution) to a constant factor equal one and consequently, Y becomes $N(m, \sigma^2)$ in the limit. The mean and variance of a Laplace variable are also given respectively by

$$\mathsf{E}\left[Y\right] = m \;\text{ and }\; \mathsf{V}\left[Y\right] = \sigma^2. \tag{4}$$

We refer to [11] for a comprehensive treatment of the generalized Laplace distributions.

Although the Laplace distribution often fits the empirical records quite well, the constant variance over data segments has an additional difficulty in the need to impose a model for the lengths of the constant variance segments. The simplest model assuming equally spaced segments and independent variances usually cannot be adopted since it is observed, not surprisingly, that variances of adjacent parts of the record are typically correlated. To circumvent this problem effectively, we use the above ideas by building a simple model that does not require ad hoc splitting of the data into segments. Namely, it is reasonable to believe that the quality of road as measured by variance varies slowly and hence the variances are likely dependent between themselves. It would then be appropriate to model them by means of an autocorrelated model. Hence, a combination of an autoregressive gamma model for variances with a classical Gaussian autoregressive models results in a flexible non-Gaussian time series defined by only five parameters, mean m, variance σ^2, shape ν and two autoregressive parameters, ρ_x and ρ_r.

Empirical example - slopes of a road in a mine

The presented Laplace time series model will be illustrated using measured slopes of a 33 km long segment of rough road surface in a mine. The slopes are measured in % and sampled each 20 meters.

The data are presented in Figure 1. In the figure, sections with almost constant variance are marked by the vertical lines. The signal has mean zero, variance 14.18 and kurtosis 6.32. In Figure 2 the normalized histogram of the measured slopes is compared with the probability density functions (pdf) of the normal model $N(0, 14.18)$ and the generalized Laplace pdf defined in (5) with parameters $m = 0$, $\sigma^2 = 14.18$ and $\nu = 1.108$. We observe that the Laplace distribution adequately represents the empirical distribution of the data. As it is shown in the next sections, variances of slopes can be fitted fairly well by the autoregressive gamma process.

3 Autoregressive gamma variance AR(1) model

The key property of the autoregressive gamma variance model is that it introduces the dependence to the random gamma variance scaling in (1) with a single parameter that control the degree of the dependence. The two features of the model need to be emphasized: firstly, it preserves the generalized Laplace distribution of the data; secondly, it replaces the concept of segments with constant variances by introducing the dependence between varying variances. In this way, the problematic issue of identifying intervals of constant variance is replaced by straightforward estimation of a single parameter that controls the lag of dependence. It is worth to mention that the model has also extension to account for asymmetry in data distribution.

Here is how the symmetric model for the slopes Y_k is formally introduced, in which we follow,

$$Y_k = \sigma \sqrt{R_k}\, X_k + m \tag{5}$$

where X_k's follow the Gaussian AR(1), while R_k's are gamma autoregressive random variables independent of X_k's. The model was first considered in [8], where it was used in a model of parallel tracks. These two components of the model are described below in further details. Figure 3 illustrates the capacity of the model to account for varying variance. In the top graph, we can see a simulated record with segments of clearly different variabilities, resembling records in Figure 1. In the bottom graph, we see the corresponding random variance itself.

In our application, the gamma factors R_k's reflect the variability of the road hilliness while the Gaussian process X_k models the local variability of the slopes. It should be emphasized that our restriction to the AR(1) model for X_k is because of simplicity and one can also consider, for example, higher order of autoregressive Gaussian processes. The model will be used to describe the variability of the slopes of a road in a mine shown in Figure 1. Due to the intended simplicity, the proposed stationary time series model does not attempt to capture all aspects of the measured signals. Our focus is on modeling the long-term distribution of some properties relevant for fuel consumption, e.g. length, height and average steepness of hills.

Autoregressive gamma model for R_k

In our application, the gamma factors R_k's model the variability of the variance of slopes in Y_k. The quality of a surface varies slowly and hence the factors R_k's are likely dependent between consecutive parts of the road. As reported in [8], the stationary gamma process R_k, with correlation coefficient ρ_r and shape ν can be written as

$$R_k = \rho_r\, K(R_{k-1}) \cdot R_{k-1} + (1 - \rho_r)\, \epsilon_k, \tag{6}$$

where $\rho_r \in (0, 1)$ is an autoregressive coefficient, ϵ_k's are mutually independent gamma distributed variables – random innovations – with mean one and variance equal to the parameter ν, independent also from $K_k = K(R_{k-1})$ and R_{k-1}. Here the random factor $K(r)$ is given by

$$K(r) = \frac{1}{m(r)} \sum_{i=0}^{N(r)} E_i, \tag{7}$$

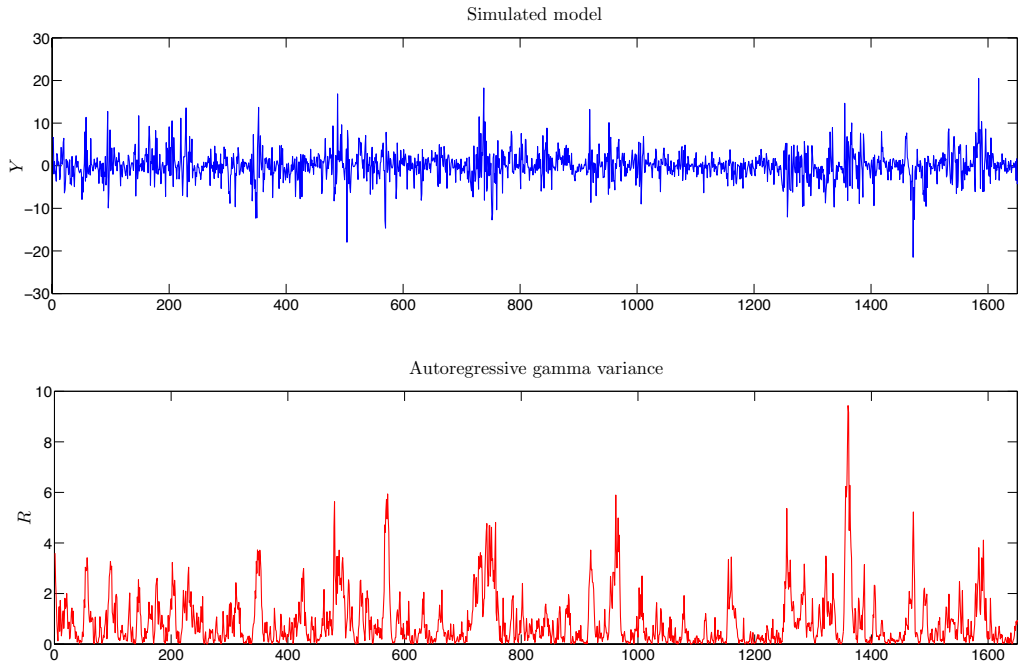

Figure 3: *Top*: Simulated values of Y. *Bottom*: Corresponding simulated values of autoregressive gamma variance.

where E_i's are independent random variables, $E_0 = 0$ while, for $i > 0$, E_i's are exponentially distributed and independent of the Poisson random variable $N(r)$ having mean $m(r)$ equal to

$$m(r) = \frac{\rho_r}{1-\rho_r}\frac{r}{\nu}. \tag{8}$$

It has been shown that this model has exponentially decaying autocorrelation ρ_r^k, $k = 0, 1, \ldots$, see [16], where the gamma autoregressive model has been introduced, or [12], where a historical overview and further properties of this model are presented.

Gaussian AR(1) time series for X_k

While an arbitrary stationary Gaussian time series X_k leads to a generalized Laplace distribution for Y_k, we restrict ourself to the autoregressive X_k of order one with the autocorrelation function $\rho_X(k) = \rho_x^k$, $\rho_x \in (-1, 1)$, normalized so that variance equals to one. We have the following classical recursive formula

$$X_k = \rho_x X_{k-1} + \sqrt{1-\rho_x^2}\,\varepsilon_k, \tag{9}$$

where ε_k's are independent zero mean Gaussian variables with variance one (Gaussian white noise). The parameter ρ_x completely determines the joint distribution of X_k's. We note that the vector process (X_k, R_k) has the Markov property, while Y_k, defined in (5) as a function of (X_k, R_k) is not a Markov process, anymore.

4 Autocorrelation functions

One approach to estimation of the parameters that govern correlation structures is to consider sample correlation estimates and matching them with the theoretical ones. For this one has to derive the formulas for autocorrelations of some functions defined on the process. For our model two autocorrelation functions are of interest: $\rho_{y^2}(k) = \text{corr}\left(Y_k^2, Y_0^2\right)$ and $\rho_y(k) = \text{corr}\left(Y_k, Y_0\right)$, $k = 0, 1, 2, \ldots$. In the

case of process Y_k centered at zero, Y_k^2 can be viewed as a local estimate of the variance, and thus $\rho_{y^2}(k)$ should roughly represent the dependence of the random variance R_k. Thus, the autocovariances of the squared records should serve well for estimation of the parameter ρ_r. On the other hand, the covariance of the Gaussian part of the model, i.e. the process X_k should be more evident in the covariance of $\rho_y(k)$. These claims are formalized in the following result, where we provide explicit formulas for autocorrelations, while their derivation is elaborated in the appendix.

Proposition 1. *For the model Y_k given in (5) with R_k and X_k following (6) and (9), respectively, we have*

(i) the autocorrelation of non-negative process Y_k^2 is given by

$$\rho_{y^2}(k) = \frac{2\rho_x^{2k} + (2\rho_x^{2k}+1)\nu\,\rho_r^k}{2+3\nu}. \tag{10}$$

(ii) the autocorrelation of process Y_k is given by

$$\rho_y(k) = (a_\nu + (1-a_\nu)\rho_{r^{1/2}}(k))\,\rho_x^k, \tag{11}$$

where

$$a_\nu = \nu\frac{\Gamma^2(\frac{1}{\nu}+\frac{1}{2})}{\Gamma^2(\frac{1}{\nu})} \tag{12}$$

and $\rho_{r^{1/2}}(k)$ is the autocorrelation of $R_k^{1/2}$.

The autocorrelation $\rho_{r^{1/2}}(k)$ of $\sqrt{R_k}$ depends on ρ_r and also on ν, so it can be formally written as a certain function $h(\rho_r,\nu,k)$, $\rho_r\in(0,1)$, $\nu>0$, $k=1,2,\ldots$. A general explicit form of $h(\rho_r,\nu,k)$ is rather difficult to obtain. Here we present only the case $k=1$:

$$\begin{aligned} h(\rho_r,\nu,1) &= \frac{\Gamma^2(\frac{1}{\nu}+\frac{1}{2})\left((1-\rho_r)^{\frac{1}{\nu}+1}\cdot F_{\frac{1}{\nu}+\frac{1}{2},\frac{1}{\nu}+\frac{1}{2},\frac{1}{\nu}}(\rho_r)-1\right)}{\Gamma(\frac{1}{\nu})\Gamma(\frac{1}{\nu}+1)-\Gamma^2(\frac{1}{\nu}+\frac{1}{2})} \\ &= \frac{a_\nu}{1-a_\nu}\left((1-\rho_r)^{\frac{1}{\nu}+1}\cdot F_{\frac{1}{\nu}+\frac{1}{2},\frac{1}{\nu}+\frac{1}{2},\frac{1}{\nu}}(\rho_r)-1\right), \end{aligned} \tag{13}$$

where $F_{a,b,c}(z)$ is a hypergeometric function defined as

$$F(a,b;c;z) = \sum_{n=0}^{\infty}\frac{(a)_n(b)_n}{(c)_n}\frac{z^n}{n!},$$

where $(q)_n$ is the (rising) Pochhammer symbol. We note that for most practical purposes, one can use a simpler approximate relation. Namely, Figure 4 *(left)* shows the behavior of $h(\rho_r,\nu,1)=\rho_{r^{1/2}}(1)$ in terms of different ν and ρ_r. Since the deviation of $\rho_{r^{1/2}}(1)$ from ρ_r is very small (with the maximal error of approximation reaching 0.0464), one can simply use ρ_r instead of $\rho_{r^{1/2}}(1)$, with the approximation error illustrated in Figure 4 *(Right)*.

From (11), in the case of $k=1$, we get

$$\rho_y(1) = a_\nu\,(1-\rho_r)^{\frac{1}{\nu}+1}\,F_{\frac{1}{\nu}+\frac{1}{2},\frac{1}{\nu}+\frac{1}{2},\frac{1}{\nu}}(\rho_r)\,\rho_x,$$

where a_ν is given in (12). However, we saw in Figure 4 that there is a quite range of parameters which this relation can be approximated by

$$\rho_y(1) = (a_\nu + (1-a_\nu)\rho_r)\rho_x. \tag{14}$$

Finally, we note that while both X_k and R_k have AR(1)-type correlations, the autocorrelation function $\rho_y(k)$ of Y_k is not of an exponential form ρ_x^k except in the case when $\rho_r=0$. In this latter case

$$\rho_y(k) = a_\nu\rho_x^k, \quad \text{if} \quad k>0. \tag{15}$$

In this special case, there is a jump in autocorrelation at $k=0$ and this property can be used for detection if the simplified model is applicable to the data.

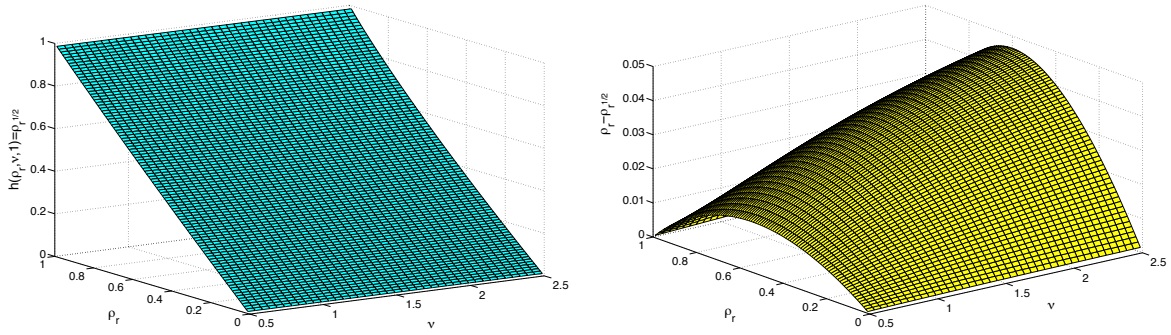

Figure 4: *Left:* Graph of $h(\rho_r, \nu, 1) = \rho_{r^{1/2}}(1)$ as a function of ν and ρ_r. *Right:* Graph of difference of $\rho_{r^{1/2}}(1)$ and ρ_r.

5 Estimation of model parameters

The model (5) has all together five parameters, the center m, the scale σ, the shape parameter ν and two one-step correlations, ρ_r and ρ_x. Estimation of the center m and the scale σ can be done in the standard way, i.e. by taking the sample mean and sample standard deviation. From now on, we assume that our data are standardized so we can assume that $m = 0$ and $\sigma = 1$ and our goal is to estimate the remaining three parameters: the shape parameter ν and the two correlations, ρ_x and ρ_r. Parameter ν can be obtained from matching sample excess kurtosis with ν via (3), which reduces the problem to estimation of the two one-step correlations, ρ_r and ρ_x.

5.1 Autocorrelation method

Fitting ρ_x and ρ_r can be obtained through fitting the covariances of Y and Y^2. The method is based on the equations (11) and (17). The formula for the one lag autocorrelation of Y can be used to establish a relation between ρ_x and ρ_r. Namely, for a sample estimate $\hat{\rho}_y$ of one step correlation of the data, we can set the equation

$$\hat{\rho}_y = ((1 - \hat{a})h(\rho_r) + \hat{a})\,\rho_x,$$

where $\hat{a} = a_{\hat{\nu}}$ and $h(\rho) = h(\rho, \hat{\nu}, 1)$ is given by (13). To make the relation even simpler, one can use approximated relation (14) to obtain the explicit relation

$$\rho_x = \frac{\hat{\rho}_y}{\hat{a} + (1 - \hat{a})\rho_r}. \tag{16}$$

Let us now introduce a function

$$G_k(\rho) = \frac{1}{\nu}\left(\frac{1 + (3\nu + 2)\rho_{y^2}(k)}{2\rho^{2k} + 1} - 1\right). \tag{17}$$

Based on (10), the function G_k should be equal to ρ_r^k when it is evaluated at $\rho = \rho_x$. Consequently, we have the possibility of using (17) to match ρ_r with the empirical evidence, by replacing ρ_{y^2} by the standard sample estimate of the autocorrelation of the squared values of the signal. Then, using the right hand side of (17), one can use sample estimates $\hat{\rho}_{y^2}(k)$ of $\rho_{y^2}(k)$ to obtain functions $\widehat{G}_k(\rho_x)$, $k = 1, \ldots, K$ of the yet undetermined ρ_x. The value of the maximal lag K should be chosen not too large so that at this lag there is still some meaningful dependence in the data. Since these functions should be approximately equal to ρ_r^k, we set them equal to one when $\widehat{G}_k(\rho_x)$ exceeds one and to zero when it is smaller than zero. Further, if we use (16), this function becomes a function of ρ_r, denoted now by $H_k(\rho_r)$:

$$H_k(\rho_r) = \widehat{G}_k\left(\frac{\hat{\rho}_y}{\hat{a} + (1 - \hat{a})\rho_r}\right). \tag{18}$$

An estimate of ρ_r can be found by solving in ρ:

$$\rho^k = H_k(\rho).$$

The solutions, say $\hat{\rho}_{rk}$, can be combined through a weighted geometric average with linearly decreasing weights

$$\hat{\rho}_r = \left(\hat{\rho}_{r1}^K \hat{\rho}_{r2}^{K-1} \dots \hat{\rho}_{rK}\right)^{\frac{2}{K(K+1)}}.$$

Finally, $\hat{\rho}_r$ can be plugged into (16) to get the corresponding estimate $\hat{\rho}_x$ of ρ_x.

We note that the above fitting method is suitable when the Gaussian component is characterized by one parameter, as it is the case in our AR(1) model. For more general Gaussian components, one can alternatively use the one-step correlation formula for Y_k to relate ρ_r with $\rho_x(1)$ and then use (22) in the appendix to fit $\rho_x(k)$, for more general models of $\rho_x(k)$.

5.2 Zero-crossing method

The Gaussian component X is characterized by a single parameter ρ_x. Since in our process the factors $\sqrt{R_k}$ are strictly positive, the observed zero crossings coincide with the zero crossings of X; the property that can be used to estimate ρ_x. In other words, we can utilize an important characteristic of the time series of slopes – the frequency of encountered hills f (in the sampling frequency unit) is defined as follows.

Let N_n be the number of encountered hills, i.e. the number of times that Y_k up-crosses level zero for $k = 0, \dots, n$. Then the (dimensionless) frequency is defined as

$$f = \lim_{n\to\infty} \frac{N_n}{n} = \lim_{n\to\infty} \frac{\#\{i = 1, \dots, n-1 : Y_i < 0, Y_{i+1} > 0\}}{n},$$

where $\#A$ denotes number of elements in a set A. For the slopes Y_k, defined in (5), the frequency of hills is equal to the frequency of zero upcrossings in the Gaussian time-series X_k. Now, for a zero mean stationary and ergodic Gaussian time series, the frequency of zero upcrossings is given by

$$f = \mathsf{P}(X_1 < 0, X_2 > 0) = \frac{1}{4} - \frac{1}{2\pi} \arcsin \rho_x, \tag{19}$$

which is the special case $\alpha = 0$, $\beta = 0$ of a general relation for standardized jointly Gaussian variables X and Y with correlation ρ:

$$\mathsf{E}\left[X^{+\alpha} Y^{-\beta}\right] = \frac{\Gamma\left(\frac{\alpha+\beta}{2} + 1\right) 2^{\frac{\alpha+\beta}{2}}}{2\pi} \left(1 - \rho^2\right)^{\frac{\alpha+\beta+1}{2}} \int_0^{\pi/2} \frac{\cos^2\phi \cdot \sin^\beta \phi}{\left(1 - \rho \sin(2\phi)\right)^{\frac{\alpha+\beta}{2}+1}} \, d\phi,$$

that can be found in [1]. Here $x^+ = \max(0, x)$ while $x^- = \max(0, -x)$. One can use (19) by taking $\hat{\rho}_x$ matching the empirically observed frequency

$$\hat{f} = \frac{\#\{i = 1, \dots, n-1 : Y_i < 0, Y_{i+1} > 0\}}{n},$$

giving

$$\hat{\rho}_x = -\sin(2\pi(\hat{f} - 0.25)). \tag{20}$$

Once the estimation of ρ_x is concluded, one can substitute the estimate of ρ_x in (10) and estimate ρ_r by fitting it to the empirical correlation $\hat{\rho}_{y^2}(k)$. Namely, the resulting

$$\hat{\rho}_{rk} = \left[\widehat{G}_k(\hat{\rho}_x)\right]^{1/k}, \; k = 1, \dots, K,$$

are used to match ρ_r. There are many ways to do so, since we have a sequence of values and only one parameter ρ_r to match them. Since the accuracy of these estimators depends and generally decreases

Table 1: Estimation of ν, ρ_x and ρ_r for two trajectory lengths: 1500 – roman, and 10000 – italics. The numbers represent Monte Carlo approximation of the mean values of the estimates (in the parentheses are the standard deviation of the estimates) based on independent samples of size 20 and lag $K = 3$

Parameters			**Estimators**				
				Autocorrelation mehtod		Zero-crossing method	
ν	ρ_x	ρ_r	$\hat{\nu}(\hat{\sigma}_{\hat{\nu}})$	$\hat{\rho}_x$	$\hat{\rho}_r$	$\hat{\rho}_x$	$\hat{\rho}_r$
1	0.6	0.7	0.93 (0.21)	0.60 (0.04)	0.57 (0.19)	0.60 (0.04)	0.58 (0.20)
			1.02 (0.12)	*0.60 (0.01)*	*0.70 (0.06)*	*0.60 (0.01)*	*0.69 (0.05)*
		0.9	0.87 (0.25)	0.60 (0.03)	0.83 (0.06)	0.59 (0.03)	0.87 (0.11)
			0.96 (0.12)	*0.60 (0.01)*	*0.89 (0.08)*	*0.60 (0.01)*	*0.89 (0.09)*
	0.8	0.7	0.87 (0.22)	0.80 (0.02)	0.63 (0.12)	0.78 (0.03)	0.66 (0.10)
			1.00 (0.10)	*0.79 (0.01)*	*0.74 (0.06)*	*0.80 (0.01)*	*0.72 (0.06)*
		0.9	0.98 (0.42)	0.82 (0.05)	0.82 (0.16)	0.81 (0.02)	0.85 (0.11)
			1.05 (0.16)	*0.80 (0.02)*	*0.88 (0.07)*	*0.80 (0.01)*	*0.90 (0.06)*
2	0.6	0.7	1.76 (0.43)	0.58 (0.05)	0.68 (0.13)	0.59 (0.03)	0.68 (0.14)
			2.04 (0.26)	*0.60 (0.02)*	*0.70 (0.08)*	*0.60 (0.01)*	*0.71 (0.07)*
		0.9	1.84 (0.49)	0.62 (0.04)	0.81 (0.10)	0.60 (0.03)	0.86 (0.11)
			1.90 (0.28)	*0.60 (0.02)*	*0.88 (0.07)*	*0.59 (0.01)*	*0.91 (0.06)*
	0.8	0.7	1.92 (0.44)	0.78 (0.06)	0.69 (0.15)	0.75 (0.02)	0.74 (0.14)
			1.95 (0.18)	*0.79 (0.03)*	*0.69 (0.09)*	*0.78 (0.02)*	*0.70 (0.07)*
		0.9	1.58 (0.53)	0.81 (0.05)	0.79 (0.13)	0.78 (0.04)	0.84 (0.12)
			1.95 (0.39)	*0.79 (0.01)*	*0.90 (0.06)*	*0.79 (0.01)*	*0.91 (0.05)*

with k, the fitting procedure should account for this effect. Here, we take a simple approach again using the weighted geometric average with linearly decreasing weights to combine the solutions

$$\hat{\rho}_r = \left(\hat{\rho}_{r1}^K \hat{\rho}_{r2}^{K-1} \dots \hat{\rho}_{rK}\right)^{\frac{2}{K(K+1)}} . \tag{21}$$

It is worth to note that the method described in the previous subsection did not use the observed frequency of hills which were used here to estimate ρ_x. Consequently, by combining the previous approach with the zero-crossing method one can, in principle, fit models for which autocorrelation of X involves two parameters. Such more general models are not considered in this work.

5.3 Comparisons of the estimation methods

For verification of the proposed estimation procedures, we simulate data points from the model using different combinations of parameters ν, ρ_x and ρ_r. From this we obtain Monte Carlo approximation of the mean values and standard deviations of the estimates. Two different trajectories of length 1500 and 10000 are considered and ensuing results are shown in Table 1.

The results are satisfactory and comparable for both methods with acceptable variances of the estimators. Although the estimation accuracy is better for longer trajectory, it is still acceptable even for the sample size of $n = 1500$. Since we deal here with fairly dependent data, estimation accuracy will largely depend on the strength of the dependence in the data – closer ρ_x and ρ_r are to one more data is needed to estimate these parameters. In both of the *zero-crossing* and *autocorrelation* methods, estimation of ρ_x performs similarly. For lower values of ρ_r, the *autocorrelation* method estimates ρ_r accurately. For higher values of ρ_x and ρ_r, the *zero-crossing* method appears to be better. Variances for estimates of ρ_r are quite comparable and in some cases somewhat smaller for the *zero-crossing* method but evidence is not compelling. In addition, the value of ν parameter has not any significant effect on the estimation of ρ_x and ρ_r but the estimate of ν is quite variable and appears to be slightly biased

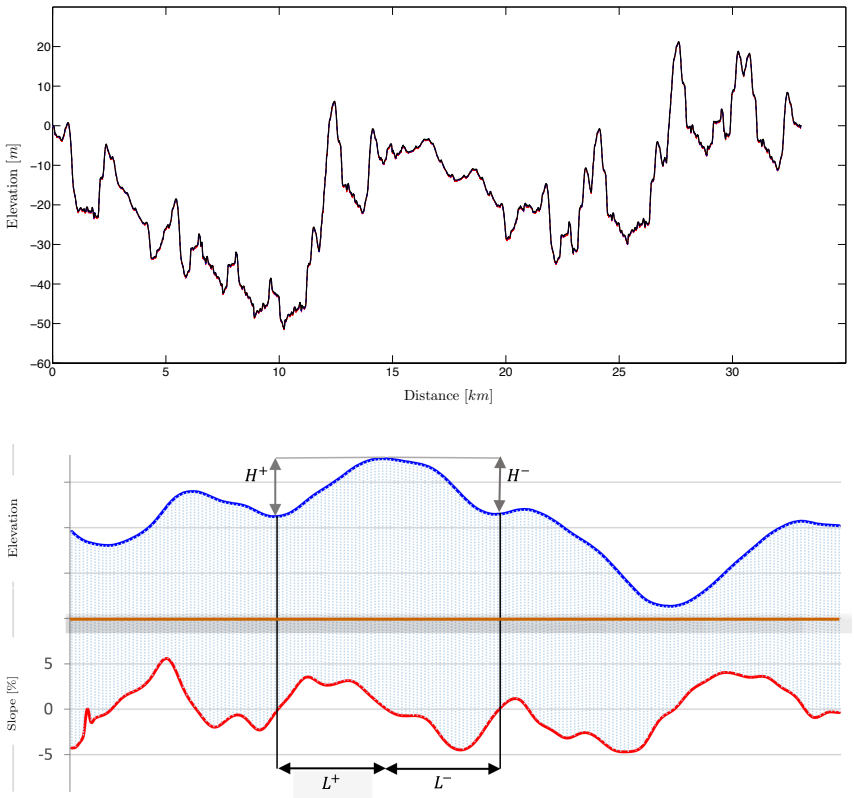

Figure 5: *Top*: The topography (elevation in $[m]$) of the road. *Bottom*: Graphical demonstration of defined hilliness characteristics.

for the larger ν and ρ_r. These are preliminary findings and more studies are needed to confirm these observations.

6 Modeling slopes in a mine

Here the Laplace autoregressive model is used to describe a real road topography data set. In Figure 2 it was shown that the long term distribution of encountered slopes is well described by means of a generalized Laplace distribution. It is rather unreasonable to expect that the complex dependence in the actual data can be described completely by our simple model. While, as mentioned before, it is possible to consider a more complicated Gaussian component, the goal here is to examine how well our two parameter dependence model captures the important hilliness characteristics encountered in the road profile, see Figure 5 *(Top)*.

6.1 Hilliness characteristics

In order to discuss properties of our random model for slopes variability, road topography and, in particular, variability of their hilliness, there is a need for a mathematical definition of some characteristics of the road topography. These definitions are represented graphically using a portion of hilliness data in Figure 5 *(Bottom)*.

A hill starts when the slope becomes positive and continues as long as one drives upwards to the crest. Then slope becomes negative and a hill continues until the slope becomes positive again and the next hill starts. Mathematically speaking, a hill is a part of a sequence of slopes Y_k, say, between two consecutive upcrossings of zero level by Y_k. The horizontal length of a hill is the distance between

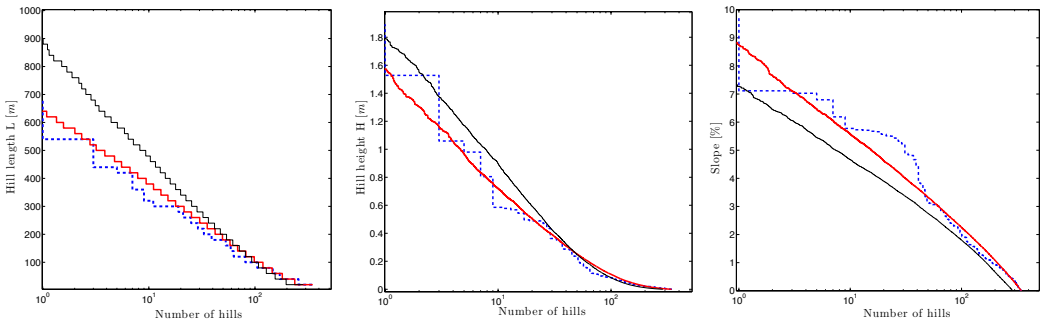

Figure 6: Comparison of amplitude spectra of hill lengths L *(Left)*, hill heights H *(Middle)* and average slopes S *(Right)* encountered in the actual data (dashed lines) and in simulated ones. Simulated Y_k process is defined by fitted parameters. The zero-crossing method is represented by thick lines and the autocorrelation method by the thin lines.

two consecutive upcrossings. Here we split a hill in the part where road goes up (uphill) and the part when it goes down (downhill). The length of the two parts are denoted by L^+ and L^-, respectively. The steepness is described by averaging slopes. Namely, S^+ is the average slope on the uphill while S^- is the average slope on the downhill. Clearly, a hill height is $H^+ = 0.01 \cdot S^+ \cdot L^+$ on the uphill side and $H^- = 0.01 \cdot S^- \cdot L^-$ on the downhill side (S is measured in $\%$). We aim to find a model of the time series of slopes Y_k which theoretically provides distribution of the hills characteristics. Since the model is symmetric, the model characteristics L^+, S^+, H^+ will have the same distribution as L^-, $-S^-$ and $-H^-$, respectively. For simplicity of the presentation, in the following we will only consider characteristics L^+, S^+, H^+ and denote them by L, S, H, respectively. We shall demonstrate that the important hill characteristics; horizontal length L, average slope S, and vertical height H are reasonably well modeled by means of the introduced model.

Distributions of hill characteristics are compared using the so-called amplitude spectrum that is defined as follows. Suppose that we have a sequence of positive quantities (amplitudes) $z_i > 0$, $i = 1, \ldots, n$. The observations have the cumulative distribution function (cdf) $F_Z(z)$. To illustrate the distribution of z_i, instead of plotting the pairs $(z, F_Z(z))$, one can alternatively use the amplitude spectrum which is a graph of $(n\,(1-F_Z(z)), z), z \geq 0$. In a plot of amplitude spectra of two sequences, one can verify whether the signals have the same distribution of large to moderate amplitudes. This is often used in fatigue analysis to compare two sequences of cycles amplitudes, see e.g. [10].

6.2 Hilliness characteristics using the zero-crossing method

Variability of L - estimation of the parameter ρ_x

We begin with the horizontal length L that is completely determined by time series X_k, i.e. a Gaussian AR(1) process having parameter ρ_x. Since the records are measured every $20[m]$, the estimated intensity of hills is $\hat{f}/20 = 0.0053\ [m^{-1}]$ which gives $\mathsf{E}\,[L] = 10/\hat{f} = 94.9[m]$ and also, by (20), $\rho_x = 0.79$. We turn next to comparison of the variability of L_i found in the measured signal and extracted from a simulation of 100 Gaussian AR(1) processes of the same length as the measured signal. In Figure 6 *(Left)*, the dashed line represents the amplitude spectrum of the observed horizontal lengths L_i, $i = 1, \ldots, n$. The amplitude spectra from 100 simulations for the horizontal lengths of the hills each fit by the zero-crossing method have been averaged and presented using thick lines. We observe a quite good agreement between the model and the empirical amplitude spectrum for the zero-crossing method marked by the thick solid line. In this figure it is also marked by the thin line, the corresponding amplitude spectra for the autocorrelation fit to the data. The result shows that the autocorrelation fitting slightly overestimates sizes of the hill lengths.

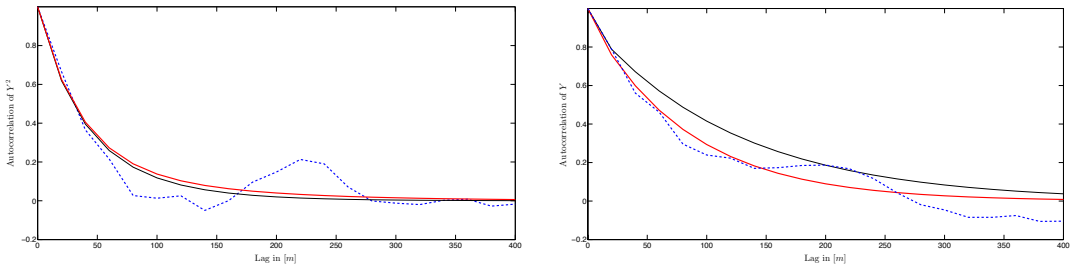

Figure 7: Comparison of the autocorrelations $\hat{\rho}_{y^2}(k)$, $\hat{\rho}_y(k)$, *left*, *right* plots respectively, fitted to the data presented in Figure 1. The thick dashed lines are the empirical autocorrelations. The thin solid lines are the theoretical autocorrelations of the introduced model with parameters $\rho_x = 0.852, \rho_r = 0.679$ fitted using the autocorrelation method, while in thick solid lines, the fit obtained from the zero-crossing method yields parameters $\rho_x = 0.789, \rho_r = 0.839$ and is presented .

Variability of S and H - estimation of the parameter ρ_r

Since the correlation ρ_x is already estimated in the previous section, it remains to fit ρ_r. For this, we use relation (10) in which ν has be replaced by its estimated $\hat{\nu} = 1.11$ obtained from the empirical kurtosis. We apply (17) for this purpose, as described in Section 5. In our particular example, we have chosen $K = 3$, which corresponds to using autocorrelations at $20[m]$, $40[m]$, and $60[m]$ – a reasonable choice of lags for the topography records. This has yielded $\hat{\rho}_r = 0.84$.

In Figure 7, we present the sample estimate of $\rho_{y^2}(k)$ versus the one obtained from the model using the fitted values of ρ_r and ρ_x. The fits are quite reasonable but our model does not capture all the dependencies observed in the data. This could be remedied by considering more general correlation (spectra) for the Gaussian component. This approach, however, is not explored in this paper as our simple model seems to capture well the essential topographical features of the data.

To seek confirmation of the adequacy of the fitted gamma autoregressive variance AR(1) model, we present averages of the vertical heights of hills H and the extracted slopes S based on 100 simulations. The resulting amplitude spectra are shown in Figure 6 (*Middle)* and *(Right)* using a thin line. The thick lines are amplitude spectra found in the measured signal. We observe that the model captures the distribution of the height of hills and average slope. In fact, as expected, the zero-crossing model performs better than the autoregressive model in retrieving fairly accurate amplitude spectra. Nevertheless, both the fits are fairly accurate as far as to capture the fundamental hill characteristics.

6.3 Hilliness characteristics using the autocorrelation method

As described in Section 5.1, we can alternatively use the one-step correlation formula for Y_k to relate ρ_r with $\rho_x(1)$ and then use (10) to fit $\rho_x(k)$, which might be very usefull especially for more general models of $\rho_x(k)$. The solution $\hat{\rho}_x$ to this equation has to be found numerically due to the involvement of non-linear function of ρ_r in (18). Using the autocorrelation method, we have obtained $\hat{\rho}_x = 0.85$ and $\hat{\rho}_r = 0.68$. As shown in Figure 7, autocorrelation functions are estimated in a satisfactory manner by both the methods.

7 Simulating from the model

For convenience of the reader, we present a MATLAB script to simulate the discussed model and use it to simulate samples from the model.

```
>> N=1651;
>> sy=14.18; nu=1.11;
>> rho_x=0.789; rho_r=0.839;
>> rAR=zeros(N,1); xAR=zeros(N,1);
>> riid=nu*wgamrnd(1/nu,1,N,1); xiid=wnormrnd(0,1,N,1);
```

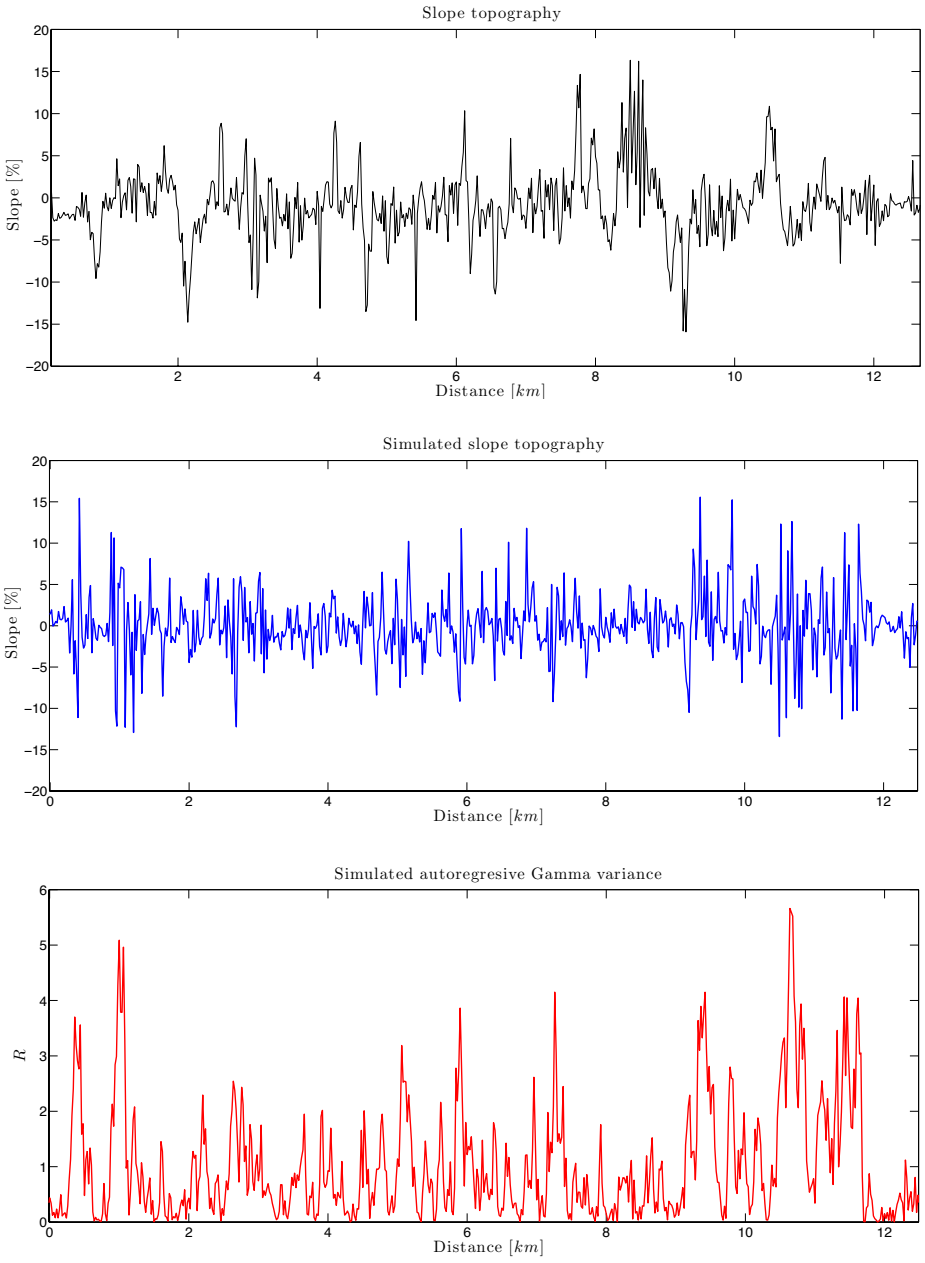

Figure 8: *(Top)*: Observed road slope topography. *(Middle)*: Simulated road slope topography. *(Bottom)*: Corresponding simulated autoregressive gamma variance. The Laplace model has the following parameters; the variance $\sigma_y^2 = 14.18$, the distributional parameter $\nu = 1.11$ and the correlations are $\rho_x = 0.789$ and $\rho_r = 0.839$.

```
>> rAR(1)=riid(1); xAR(1)=xiid(1);
>> for i=2:N
>> m=rho_r/(1-rho_r)/nu*rAR(i-1);
>> NPois=poissrnd(m);
>> if NPois>0, W=wexprnd(1,NPois,1); else W=0; end
>> kj=sum(W)/m;
>> rAR(i)=rho_r*kj*rAR(i-1)+(1-rho_r)*riid(i);
>> xAR(i)=rho_x*xAR(i-1)+sqrt(1-rho_x^2)*xiid(i);
>> end
>> y=sqrt(sy)*xAR.*(sqrt(rAR));
>> y=y-mean(y);
>> plot(1:N,cumsum(y))
```

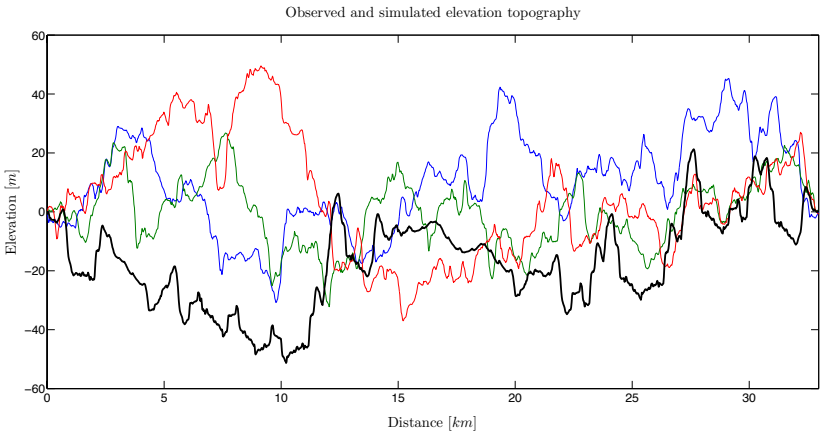

Figure 9: Three samples of simulated elevations (thin solid lines) are compared with the observed road elevation topography (solid thick line). The Laplace model has the following parameters; the variance $\sigma_y^2 = 14.18$, the distributional parameter $\nu = 1.11$ and the correlations $\rho_x = 0.789$, $\rho_r = 0.839$.

In the program the variance of Y_k, $\sigma_y^2 = 14.18$, the distributional parameter $\nu = 1.11$ while the correlations $\rho_x = 0.793$, $\rho_r = 0.839$. Using the MATLAB code, the road slope topography and the corresponding autoregressive gamma variance are simulated and plotted in Figure 8 together with the observed slope topography of a 12 $[km]$ section. The samples have the same number of points as the measured slopes in that section, i.e. $N = 621$. Using the mentioned code, three random elevation topographies are evaluated and plotted in Figure 9. The simulated topographies are compared with the observed elevation topography presented using a thick solid line. Here $N = 1621$ which corresponds to the size of the entire data set.

The changes in variability of the observed slope topography of the road are captured fairly well in the simulated slopes and also the observed elevation topography is well emulated by the model.

8 Conclusions

In the paper we discuss an extension of the classical Gaussian autoregressive models to account for non-Gaussian distribution of the records as well as to provide a more flexible representation of topography in the data of a road. The model has two components: the first one is given by a classical Gaussian AR(1) time series while the second one represents the randomly varying variance given by an autoregressive gamma process. The dependence in the model is governed by two autoregressive parameters: ρ_x for the Gaussian AR(1) part and ρ_r for the autoregressive gamma part.

The distributional parameters, location, scale and shape are obtained by fitting sample mean, variance and kurtosis to their sample equivalents. We consider two estimation methods to fit the autoregressive parameters. In the first one, the parameter ρ_x is a function of the expected length of the hills and can be simply fit using the empirical distribution of the length. The parameter ρ_r is harder to estimate since the distributions of the height of the hills and their steepness are both influenced by its value. We used a simple relation between ρ_r, ρ_x and the autocorrelation of the squared values of the slopes to obtain an estimate of ρ_r. In the second method, we have used the one-lag correlation of the slope values instead of the expected length of the hills. We illustrate that both the methods perform quite well for simulated data.

We also fit the model to an example of real-life road topography data. It is shown that the model satisfactory retrieves the distributions of the length, the average slope, and the height of the hills. The model uses only the order-one autoregressive dependence and thus is not capable of capturing longer lag dependencies that are also present in the data. This can be remedied by an extension that involves the Gaussian component with a more complex dependence structure. This direction of research will be

pursued in future.

Appendix

Autocorrelation function of Y_k and Y_k^2

The goal of this appendix is to present the argument for the theses in Proposition 1. Generally, without assuming anything except than independence between R_k and X_k, $\rho_{y^2}(k)$ is given by

$$\rho_{y^2}(k) = \frac{\rho_r(k)\rho_{x^2}(k) + \rho_r(k)cv_{x^2}^{-2} + \rho_{x^2}(k)cv_r^{-2}}{1 + cv_{x^2}^{-2} + cv_r^{-2}},$$

where $\rho_r(k) = \text{ corr}\,(R_0, R_k)$, $\rho_{x^2}(k) = \text{ corr}\left(X_0^2, X_k^2\right)$, and cv_{x^2}, cv_r are coefficients of variation for X^2 and R, respectively.

Similarly, the correlation of Y can be written as

$$\rho_y(k) = \frac{\rho_{r^{1/2}}(k) + cv_{r^{1/2}}^{-2}}{1 + cv_{r^{1/2}}^{-2}}\,\rho_x(k).$$

If we add the assumption that X_k is a Gaussian process, then we have

$$\text{Cov}\left(X_0^2, X_k^2\right) = 2\left[\,\text{Cov}\,(X_0, X_k)\,\right]^2,$$

which leads us to

$$\rho_{y^2}(k) = \frac{\rho_r(k)\rho_x^2(k) + \rho_r(k)/2 + \rho_x^2(k)cv_r^{-2}}{3/2 + cv_r^{-2}}.$$

Further, by assuming that R_k is autoregressive gamma and utilizing the formula for the moments of a gamma distribution we get $cv_r = \sqrt{\nu}$ and $\rho_r(k) = \rho_r^k$, where ρ_r is set to $\rho_r(1)$ which leads to

$$\rho_{y^2}(k) = \frac{2\nu\rho_x^2(k)\rho_r^k + \nu\rho_r^k + 2\rho_x^2(k)}{3\nu + 2}. \tag{22}$$

Similarly, since

$$cv_{r^{1/2}} = \sqrt{a_\nu - 1},$$

where

$$a_\nu = \frac{\Gamma(\frac{1}{\nu} + 1)\Gamma(\frac{1}{\nu})}{\Gamma^2(\frac{1}{\nu} + \frac{1}{2})},$$

we obtain

$$\rho_y(k) = \left[\rho_{r^{1/2}}(k) + a_\nu\left(1 - \rho_{r^{1/2}}(k)\right)\right]\rho_x(k).$$

For our special AR(1) example, it is equal to

$$\rho_{y^2}(k) = \frac{(2\rho_x^{2k} + 1)(\nu\,\rho_r^k + 1) - 1}{3\nu + 2}. \tag{23}$$

Acknowledgments

The authors are thankful to Volvo Construction Equipment for supplying data. The first and third authors were support by The Swedish Energy Agency. The research of the second and the fourth authors was supported by the Riksbankens Jubileumsfond Grant Dnr: P13-1024:1 and the Swedish Research Council Grant Dnr: 2013-5180.

References

[1] A. Baxevani, K. Podgórski, and J. Wegener. Sample path asymmetries in non-Gaussian random processes. *Scandinavian Journal of Statistics*, pages 1102–1123, 2014.

[2] K. Bogsjö. Evaluation of stochastic models of parallel road tracks. *Probabilistic Engineering Mechanics*, 22:362–370, 2007.

[3] K. Bogsjö. *Road Profile Statistics Relevant for Vehicle Fatigue*. PhD thesis, PhD thesis, Mathematical Statistics, Lund University, 2007.

[4] K. Bogsjö, K. Podgorski, and I. Rychlik. Models for road surface roughness. *Vehicle System Dynamics*, 50:725–747, 2012.

[5] B. Bruscella, V. Rouillard, and M. Sek. Analysis of road surfaces profiles. *Journal of Transportation Engineering*, 125:55–59, 1999.

[6] D. Charles. Derivation of environment descriptions and test severities from measured road transportation data. *Journal of the IES*, 36:37–42, 1993.

[7] C. J. Dodds and J. D. Robson. The description of road surface roughness. *Journal of Sound and Vibration*, 31:175–183, 1973.

[8] P. Johannesson, K. Podgórski, and I. Rychlik. Modelling roughness of road profiles on parallel tracks using roughness indicators. Technical Report 4, MV Chalmers Preprint 2014:4, 2014.

[9] P. Johannesson and I. Rychlik. Modelling of road profiles using roughness indicators. *International Journal of Vehicle Design*, pages 317–346, 2014.

[10] P. Johannesson and M. Speckert, editors. *Guide to Load Analysis for Durability in Vehicle Engineering*. Wiley-Chichester, 2013.

[11] S. Kotz, T.J. Kozubowski, and K. Podgórski. *The Laplace Distribution and Generalizations: A Revisit with Applications to Communications, Economics, Engineering and Finance*. Birkhaüser, Boston, New York, 2001.

[12] T. J. Kozubowski and K. Podgórski. Skew Laplace distributions II. Divisibility properties and extensions to stochastic processes. *Math. Scientist*, 33:35–48, 2008.

[13] M. Kvanström, K. Podgórski, and I. Rychlik. Laplace moving average model for multi-axial responses in fatigue analysis of a cultivator. *Probabilistic Engineering Mechanics*, 34:12–25, 2013.

[14] P. Mucka. Road waviness and the dynamic tyre force. *Int. J. Vehicle Design*, 36:216–232, 2004.

[15] V. Rouillard. Decomposing pavement surface profiles into a Gaussian sequence. *Int. J. Vehicle Systems Modelling and Testing*, 4:288–305, 2009.

[16] C. H. Sim. First-order autoregressive models for gamma and exponential processes. *Journal of Applied Probability*, 27:325–332, 1971.

[17] L. Sun, Z. Zhang, and J. Ruth. Modeling indirect statistics of surface roughness. *Journal of Transportation Engineering*, 127:105–111, 2001.